Vol. 41, No. 2 (2019) 143-155, DOI: 10.24874/ti.2019.41.02.01

Tribology in Industry

www.tribology.rs

RESEARCH

Effect of TiN Nanoparticles on the Friction and Wear Properties of Spark Plasma Sintered Fe-Cr-Ni

M.R. Mphahlele[a], S.R. Oke[a,b*], O.O. Ige[a,c], O.E. Falodun[a], P.A. Olubambi[a]

[a] *Centre for Nanoengineering & Tribocorrosion, School of Mining, Metallurgy & Chemical Engineering, University of Johannesburg, Johannesburg, South Africa,*
[b] *Department of Metallurgical & Materials Engineering, Federal University of Technology, Akure, Ondo State, Nigeria,*
[c] *Department of Materials Science & Engineering, Obafemi Awolowo University, Ile-Ife, Osun State, Nigeria.*

Keywords:

SAF 2205
TiN nanoparticles
Spark plasma sintering
Coefficient of friction
Wear behaviour

Corresponding author:

Samuel R. Oke
Centre for Nanoengineering & Tribocorrosion, School of Mining, Metallurgy & Chemical Engineering, University of Johannesburg,
South Africa.
E-mail: sroke@futa.edu.ng

A B S T R A C T

This study evaluated the dry sliding wear and friction behaviour of spark plasma sintered Fe-Cr-Ni (a duplex stainless steel known as SAF 2205) matrix with titanium nitride (TiN) nanoparticles as reinforcement. Tests were performed with a tribometer at a relative humidity and temperature of 50 % and 25 °C respectively. Three loads were employed for all 600 cycles tests. Thereafter, the wear mode and mechanism were microscopically examined. Results showed that the coefficient of friction for the nanocomposites were higher than that of the unreinforced SAF 2205 despite showing improved wear performance. Samples with lower TiN compositions exhibited mixed mode of wear mechanism but at higher TiN content, the adhesive mechanism prevails. This study established that increasing the addition of nanosized TiN confers better wear behaviour on spark plasma sintered SAF 2205

1. INTRODUCTION

Duplex stainless steels (DSS) are exceptional type of steel which possess characteristics that puts them on the forefront of preferred materials for numerous applications [1-2] where structural components such as rail and tire wheels, gears, rolling element bearings and valve train components are utilized. DSSs are characterized by good corrosion resistance and strength which is incomparable to that of austenitic and ferritic stainless steel [1-3]. A major concern is that DSS steels suffer considerable damage in terms of strength when exposed to aggressive wear environments [4-5]. In order to combat this drawback, several researchers have incorporated ceramic particles into stainless steel matrices [5-9]. SAF 2205 duplex stainless steel is favored in this study because it is most widely used in industrial applications where corrosion resistance and high strength is demanded [1-3].

The SAF 2205 steel in this work is produced via spark plasma sintering and reinforced with varying amount of TiN. The choice of this

processing route is favored by low process temperature, short sintering time, high heating rates, products with high density, and reduction in undesirable vaporization [10] It is imperative to state that works on the alloying of nanoceramic particles in duplex steel for improved wear resistance is scarce in literature.

In a study carried out, Jin et al. [5] examined wear behavior of TiC reinforced stainless steel cermets. It was reported that the cermets demonstrated a transition in the primary wear mechanism when higher loads are applied. The dynamic coefficient of friction (COF) decreases with increasing load. Also, that the specific wear rate increased linearly as the applied load increases when the reinforcement content and time of the test is constant. It has been reported that the wear rate of Al_2O_3 reinforced SAF 2205 was decreased due to significant amount of Al_2O_3 in circulating debris which acted as a stress release layer [8]. Engqvist and Axen [9] explained that constant wear rate can be maintained by the phenomena of grain fragmentation and pull-out in a situation whereby the reinforcing phase has low volume fraction in the composite. They argued further that with a composite having a larger volume fraction, the wear volume is minimal. They further stated that if the reinforcing phases are larger, under low loads the material show minimal wear volume. In most cases, this favorable effect is achieved when low metallic binder is rapidly removed exposing the hard-ceramic grains which are more resistant to wear.

Amongst many other cermets which possess exceptional anti-wear characteristics, TiN has emerged as a very promising material that can improve the wear behavior of DSS [11, 12]. An intriguing hypothesized role of TiN in DSS to improve the anti-wear properties of DSS is due to its good combination of strength to weight ratio, high specific modulus, high hardness, fatigue strength; good wear resistance, chemical inertness [5] and grain refinement capabilities [13]. A reported study [14] stated that metallic materials containing reinforcing particles usually follow classical Archard's wear relationship. This relationship states that the wear performance of metallic materials is a function of its hardness. Hence, fine-grained materials have better wear resistance than coarse-grained counterparts. However, it should also be considered that grain growth with nano particles could be avoided by careful selection of appropriate fabrication techniques [10].

In the preliminary study [12] that constitutes an integral part of this research work, the optimized sintering parameters were established to fabricate SAF 2205-TiN nanocomposites containing varied amounts of TIN. The optimum properties – densification and hardness behavior - were found for samples with sintering temperature (1150 °C), sintering time (15 min) and holding rate 100 °C/min. In further work, Oke et al. [15] studied the microstructural, corrosion and reciprocating wear properties of the nanocomposites sintered at different sintering conditions. The corrosion performance recommended was observed for sintered nanocomposites at 1100 °C for 10 min. While the nanocomposites sintered for 10 min at 1150 °C showed excellent reciprocating wear resistance.

This present study seeks to assess the tribological performance of SAF 2205 nanocomposites reinforced with TiN under varying loads with the aim to determine the TiN addition that will give optimum wear resistance. Ball/pin on disk tribometer was employed to evaluate the sliding wear behavior and the coefficient of friction of the nanocomposites. It is expected that this research will provide information on the wear mechanism that develops in the duplex steel reinforced with TiN nanoparticles. Thereafter, the wear mechanism is linked with the microstructural observations.

2. MATERIALS AND METHODS

2.1 Materials

Duplex stainless steel (SAF 2205) containing TiN nanoparticles in the range of 0 – 8 wt% at an interval of 2 wt% were used in this work, details of the compositions have already been reported by Oke et al. [11,15]. Pure SAF 2205 was used for a comparative purpose for all the undertaken tests. Duplex stainless steel powder (22 μm) was purchased from Sandvik Osprey Ltd, UK and TiN powder (20 nm) was purchased from Nanostructures and Amorphous Materials, Inc. USA. The compositions of the material used are shown in Table 1.

Table 1. Chemical composition of SAF 2205 and TiN (wt%).

Elements	C	Si	Mn	P	S	Cr	Ni	Mo	N	Ti	Fe
SAF 2205	≤0.03	≤1.0	≤2.0	≤0.03	≤0.015	22	5	3.2	0.18	-	Bal
TiN	0.03	<0.003	-	-	-	-	<0.001	-	21.91	77.83	<0.001

2.2 Powder preparation and spark plasma sintering

The powders were mixed for 8 hours at 72 rpm using a turbula mixer T2F to attain well homogenised mixture. The mixed powders were cold compacted and sintered using as automated spark plasma sintering machine (model HHPD-25, FCT GmbH Germany). The samples were sintered in vacuum using optimized pressure of 50 MPa, sintering temperature of 1150 °C, heating rate of 100 °C/min and sintering holding time of 15 min. detailed information on the optimization of the sintering parameters for the fabrication of the SAF 2205-TiN nanocomposites have been reported in our previous study [12]. Disc specimens with a diameter of 20 mm and height of 5 mm were produced.

2.3 Sample preparation

Prior to wear testing, good surface integrity of the sintered samples was obtained by careful preparation of the samples using semi-automated metallographic sample preparation equipment (Advanced Laboratory Solutions, ATM Saphir 550). The samples were ground and polished until the mirror-like surface finish was obtained using colloidal 0.2 μm fumed silica suspension in the last polishing stage. Lastly, the samples were cleaned with acetone and air-dried.

2.4 Wear testing

In this study, the ball-on-disk tribological technique was used to estimate and study the wear behaviour of the materials. ASTM G99-05 standard test method [16] was used to carry out the dry sliding wear tests with a ball-on-disk tribometer (UMT-2, Bruker, formerly known as CETR). The relative humidity and temperature were kept constant at 50% and 25 °C, respectively. ASTM 52100 steel was used as a counter-body while the disc samples were the sintered DSS nanocomposites. Various contact loads of 1N, 3N, and 5N at a different radius of 3mm, 6mm, and 9mm, respectively were employed. All tests were carried out to cover 600 cycles in an hour. Continuous monitoring of the coefficient of friction (COF) was observed throughout the test, a mean COF was determined and reported. The wear volume was determined by continuously recording the weight difference before and after each test using a very sensitive analytical weighing balance (Shimadzu AY120) which is able to weigh up to 0.0001g. The volume material loss (V) of the samples was calculated using the equation:

$$V = \frac{\Delta w}{\rho} \quad (1)$$

Where Δw= weigh before test-weight after test and ρ = density of the various nanocomposites

The wear rate (W) is then calculated using the Archard's linear wear equation [17-18]:

$$W = KF_N \quad (2)$$

where K is the wear coefficient and F_N is the applied load. K is calculated using the relation [18]:

$$\mathrm{K} = \frac{3\mathrm{HV}}{\mathrm{F_N D}} \quad (3)$$

where HV is the Vickers hardness of the softer body in contact and D is the sliding distance.

Finally, the specific wear rate, k, was determined based on the Lancaster relationship [19]:

$$\mathrm{k} = \frac{\mathrm{V}}{\mathrm{F_N}} \quad (4)$$

The tests were repeated up to three times to ensure the data accuracy and reliability.

2.5 Wear surface characterization

Scanning electron microscope (FESEM, JSM-7600F) equipped with energy dispersive spectroscopy (EDS) was employed to characterize the wear mechanisms and morphology.

3. RESULTS

3.1 Result of SAF 2205-TiN composites friction coefficient

Figure 1 depicts the relationship between the applied load and coefficient of friction (COF) of

the nanosized TiN particles reinforced SAF 2205 stainless steel. As the load increases, it was revealed that the friction coefficient decreased and this could be attributed to slither occurring at the composite/ball contact surfaces. For instances, there was a rise in contact temperature when the contact load was increased from 1 to 3 N (Figs. 1a and 1b), the temperature rise is attributed to the heat generated as a result of an increase in the area of contact between the composites and ball. It has been argued that there are materials surface softening which is associated with an upsurge in the contact temperature due to slipping action. The surface leads to pronounced slipping action which resulted in a reduction of the coefficient of friction [20-22]. Meanwhile, increasing the load to 5 N (Fig. 1c) resulted in a decline of the COF.

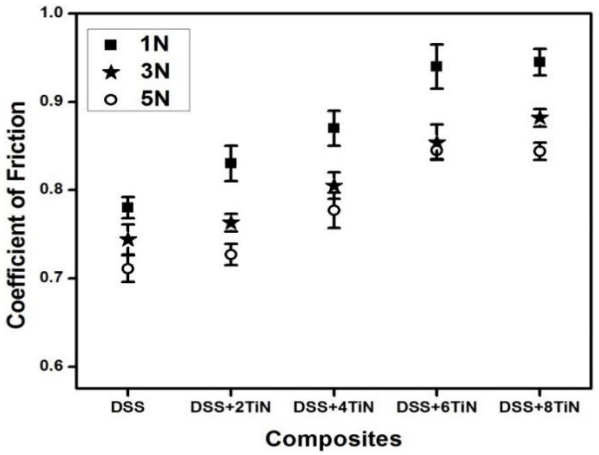

Fig. 1. Mean values of COF for unreinforced SAF 2205 and the composites based on the applied load.

The wearing of the duplex steel composite increased with applied loads, with debris forming tribolayers on the composite samples. The formation of a tribolayer on sample surface due to deformation at higher loads have been reported by Cao et al. [23], the authors elucidated that the presence of tribolayers could decrease the COF. The existence of tribolayers could hinder actual contact between the composite and the counter ball. Previous studies have reported that an increase in COF for different materials with applied loads [24-25]. Meanwhile, the COF behaves contrarily as it increases with TiN nanoparticles from 0 – 8 wt%. A distinct feature observed is that the increase in COF associated with TiN nanoparticles is not dependent on the applied load. The increase in COF could be due to the TiN nanoparticles protruding from the softer duplex steel matrix, the nanoparticles are thus pulled out during the contact and slide against each other thereby increasing the coefficient of friction [26].

3.2 Wear response of SAF 2205-TiN composites

The wear loss associated with the addition of TiN nanoparticles to duplex steel under varying loads (1, 3 and 5 N) is shown in Figure 2. It is observed that irrespective of the applied load, the wear loss decreased with TiN. A Similar trend in wear loss was noted for the composite under 3 and 5 N, the wear volume decreased with TiN up to 6 wt%, this indicates that the addition of TiN improved the wear resistance of duplex steel regardless of applied load. However, the volume of wear increased with the addition of TiN beyond 6 wt%. Literature has reported that better wear resistance is expected when the ceramic reinforcement is increased because of enhanced composite hardness [20-21, 27-28]. The increase in the volume of wear of the duplex steel containing 8 % TiN may be as a result of metallurgical defects such as vacancies, atoms clusters, and dislocations among others. These defects could act as potential weakening sites when load is applied [29]. Literature has reported a significant decrease in properties of reinforced composites with excess addition of ceramic particles [30]. The reinforcement content must be kept at a critical level so as not to affect the mechanical properties negatively. For example, Silvestre et al, reported an increase in properties with the addition of SiC nanoparticles up to 8 wt% and then significantly decreased with 12 wt% addition. The presence of porosity was stated to generally have a negative influence on the properties of the composite, due to the concentration of stress in pores, resulting in lower strength [31].

Again, from Fig. 2, it is evident that the volume of wear increased as the load increases from 1 to 5 N for all the grades of stainless steel composite. This wear loss increases linearly as the applied load which agrees with the Lancaster model [19]. The observed increase in the wear volume with applied load might be due to roughening action of the hard TiN nanoparticles. The higher amount of stress resulting from an increase in applied load causes large plastic deformation of the composite surface. Irrespective of the applied load, the optimum nanocomposite was obtained for sample containing 6 % TiN reinforcement.

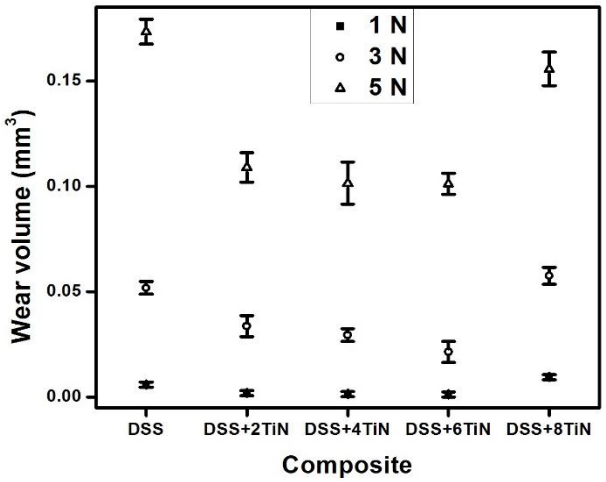

Fig. 2. The effect of TiN nanoparticle addition and applied loads on volumetric wear loss of TiN–SAF 2205 stainless steel.

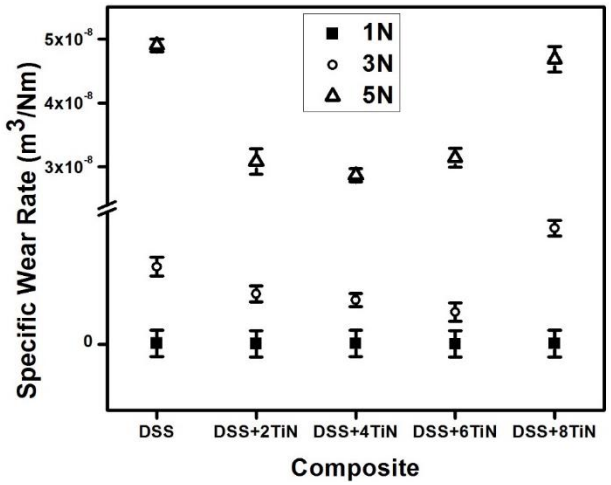

Fig. 3. The effect of TiN nanoparticle addition and applied loads on the specific wear rate of the SAF 2205 duplex stainless steel.

Wear and specific wear rates are very important parameters in engineering applications. The basic difference between the two parameters is that the wear rate (m^3/m) is independent of applied load whereas specific wear (m^3/Nm) is a function of applied load [29]. In this study, the specific wear rate is preferred. The role of applied load and TiN nanoparticles reinforcement on the specific wear rate of pure sintered duplex stainless steel and its composite are presented in Fig. 3. It is apparent that the specific wear rates decreased with the addition of TiN into a matrix of stainless steel up to 6 % reinforcement but on the contrary, it increased with applied loads from 1 to 5 N. The marked reduction of specific wear rates is an indication that the addition of TiN particles confers better performance on the nanocomposites compared to the unreinforced duplex steel irrespective of the applied loads. The implication is that increasing the content of TiN of the duplex stainless steel resulted in a linked reduction in wear rate, and this could be attributed to the high hardness/elastic modulus of the TiN phase. At higher applied loads, there is a greater amount of plastic deformation leading to higher wear rates in the samples. The wear rates obtained in our study agree in a generally positive manner to the ones reported in an earlier study [32].

3.3 Microstructural observation of the composites following sliding wear

The influence of TiN nanoparticle addition and applied loads on the morphology of the wear widths for unreinforced and reinforced stainless steel samples are presented in Fig. 4. Low magnification scale was selected in order to have better morphology of the sintered stainless steel samples. For the unreinforced duplex steel (Fig. 4), a progressive increase in wear width was observed with an increase in load from 1 to 5 N due to the relative ductility of steels. The rise in contact temperature associated with increase in applied load results in pronounce deformation of the duplex steel, this translates to an increase in wear. Comparable behaviour of increased wear track width with load is prominent for all the composite grades regardless of the amount of reinforcement. It must be noted that applied load and wear width are directly related and as such, an increase in applied load implied larger wear width [33].

However, for each of the applied load, the wear widths were noted to increase with an increase in TiN nanoparticle reinforcement (Table 2). Visual examination of the samples revealed that the wear depths of unreinforced steels were higher than those of the reinforced steel pair at each of the loads. These accounts for the reduced wear volume of the reinforced composites even though the wear widths were larger. A Plausible reason for this behaviour could be that initial damage in the reinforced steel involved minimal plastic flow with the removal of nanoparticles due to grain boundary flagging from repeated sliding, thermal expansion and elastic properties of each grain [34]. As earlier stated, the nanocomposites performed better due to the harder TiN phase which resulted in lower plastic deformation. Ultimately the wear rates were lower compared to the unreinforced samples.

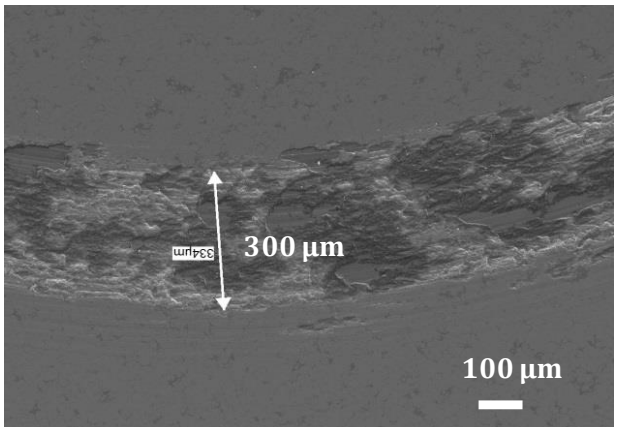

a)

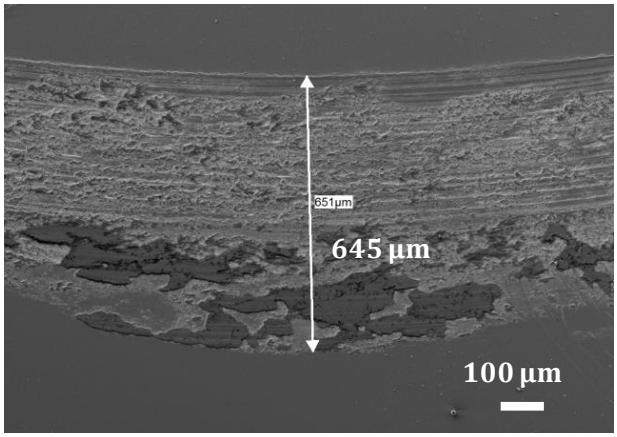

b)

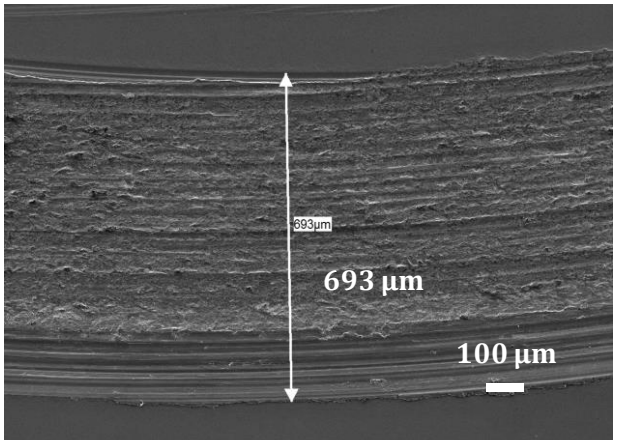

c)

Fig. 4. SEM images of the wear width configuration of unreinforced sintered SAF 2205 at (a) 1 N; (b) 3 N; and (c) 5 N, representing a trend in wear profile of the steel with or without the reinforcement.

Table 2. Summary of wear widths of the TiN nanoparticle reinforced SAF 2205 stainless steel under varying loads.

Composites	1N (µm)	3N (µm)	5N (µm)
SAF 2205	300.0	645.0	693.0
SAF 2205-2TiN	347.0	572.0	900.0
SAF 2205-4TiN	404.0	669.0	1160.0
SAF 2205-6TiN	518.0	693.0	1220.0
SAF 2205-8TiN	649.0	780.0	1170.0

The micrographs of the TiN nanoparticle reinforced duplex stainless steel samples at an applied load of 1 N were presented in Fig. 5. The micrographs are characterized with third body debris deposits on plastically – sheared surfaces. The worn surfaces for the unreinforced (Fig. 5a) and steel containing 2 wt% TiN nanoparticle (Fig. 5b) showed similar wear mechanisms. Ploughing was observed on the sample's surface, which indicates that wear proceeded by an abrasive mechanism [35]. However, due to the relatively low hardness caused by the absence of or low TiN content, spalling chips formed during the wear process were observed to adhere to the steel surface. The adhesive wear component was identified by the areas of material removal (Figs. 5a and 5b). In-depth evaluation of the wear track of the samples at 1 N applied load showed a mixed mode of adhesive–abrasive wear mechanisms. Comparing Figs. 5a and 5b, it was obvious that the extent of abrasive wear was pronounced in the unreinforced stainless steel sample (Fig. 5a). Wear volumes and wear rates were high for these grades of composite due to the excessive local ploughing of the surface as discussed in previous sections.

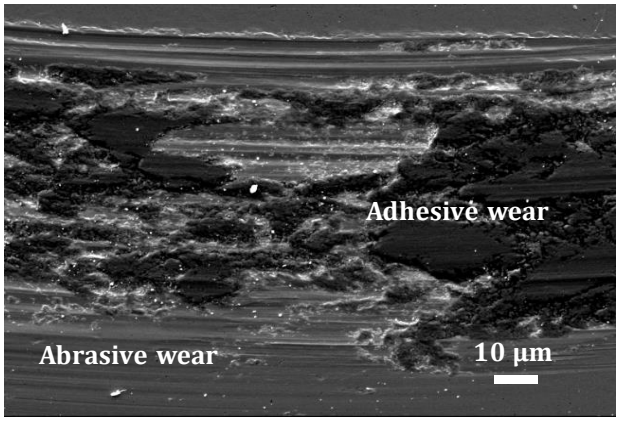

a)

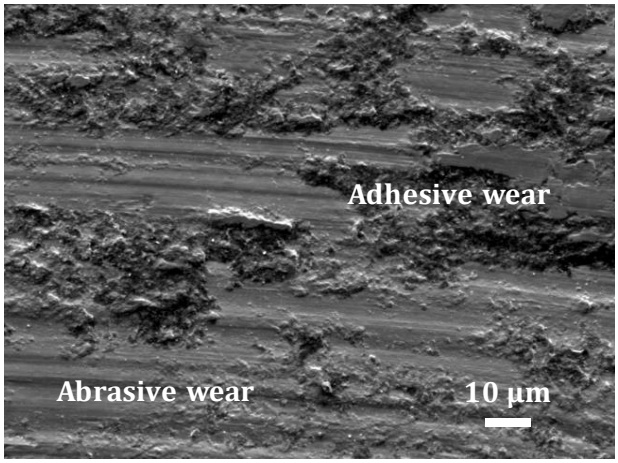

b)

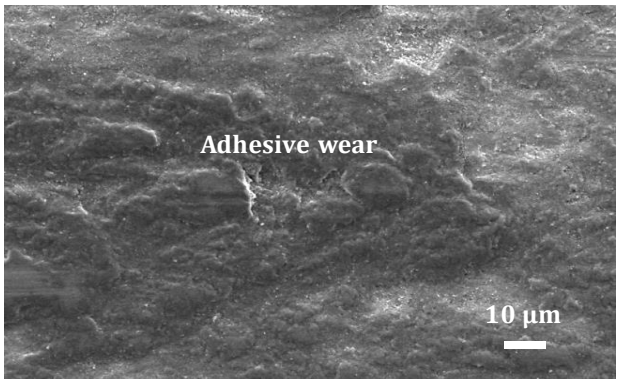

c)

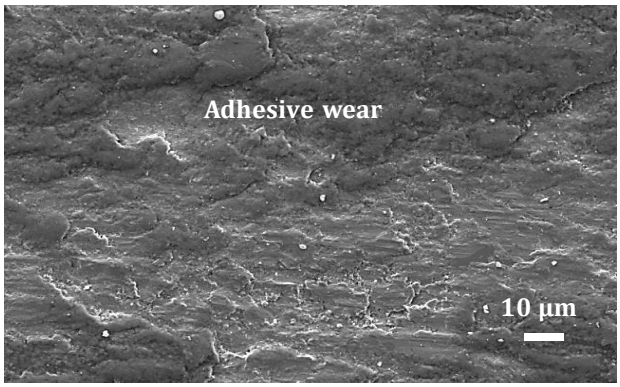

d)

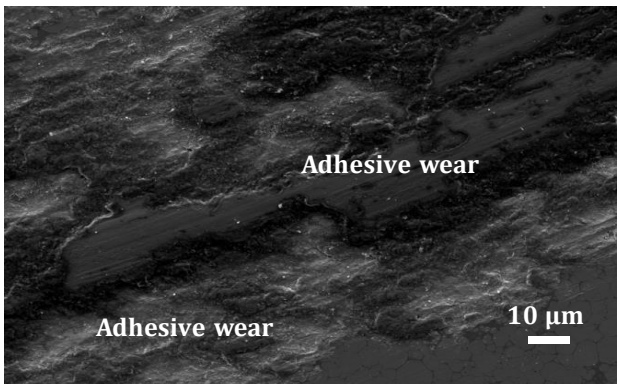

e)

Fig. 5. SEM images showing wear tracks of duplex stainless steel composite under 1 N applied load (a) SAF 2205 (b) SAF 2205 + 2TiN (c) SAF 2205 + 4TiN (d) SAF 2205 + 6TiN (e) SAF 2205 + 8TiN.

In contrast, an increase in TiN nanoparticle content of the stainless steel composite as observed in Figs. 6c and 6d, revealed that the worn surface has shallower grooves due to more compact and adhesive TiN tribolayer [35]. The formed tribolayer is smooth and less deformed compared with Figs. 6b. For these grades of composites, no protruding particles of TiN are formed and no significant ploughing or fracturing is observed on the worn surface. The adherence of TiN tribolayers on the duplex steel surface could reduce plastic deformation during wearing due to the high hardness of TiN [14].

The SEM micrographs of the worn surface of the TiN nanoparticle reinforced duplex stainless steel composite under 5 N applied load is shown in Fig. 6. For the unreinforced stainless steel sample (Fig. 6a), there is large plastic deformation. The morphology of the worn surface for stainless steel sample also showed deep ridges with scattered wear debris. The deep ridges signify that the wear occurred on the sample by abrasive mechanism, whereas the scattered wear debris is due to the adhesion wear mechanism.

The morphology characteristics were observed to be similar to that conducted at 1 N of the applied load. With the addition of nanoparticles of TiN up to 6 wt% (Figs. 6c and 6d), less worn but more plastically deformed surfaces were noticed on the sample surface. This shows that abrasive wear on the reinforced samples was less severe compared to unreinforced stainless steel sample. The argument is that the TiN nanoparticles formed compact tribolayers on the nanocomposites which reduces the wear rate by decreasing the plastic deformation. However, when TiN content is increased to 8 wt%, there is delamination of the particles on the nanocomposite surface (Fig. 6e). Also, there is pronounced micro-cracking and surface ploughing from severe abrasion.

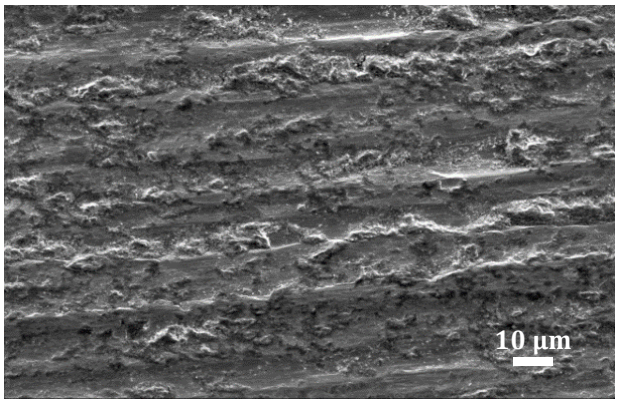

a)

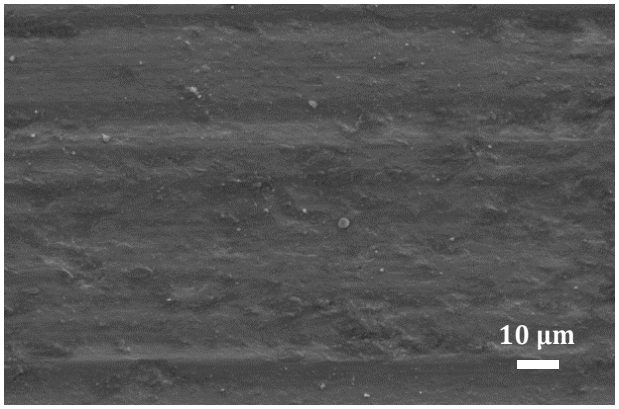

b)

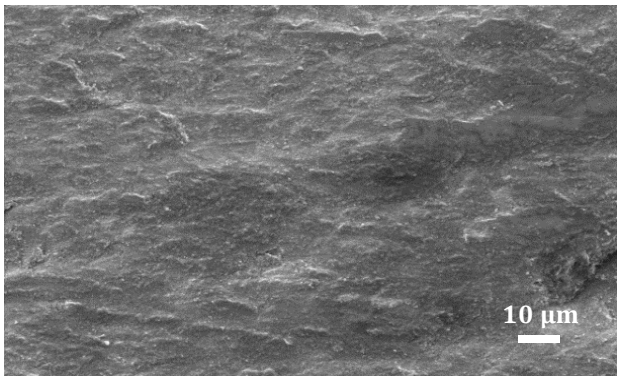

c)

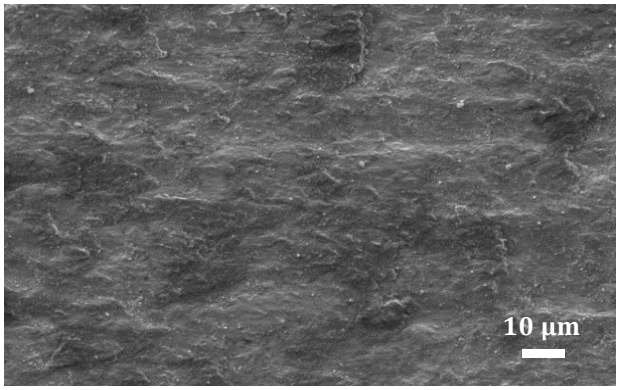

d)

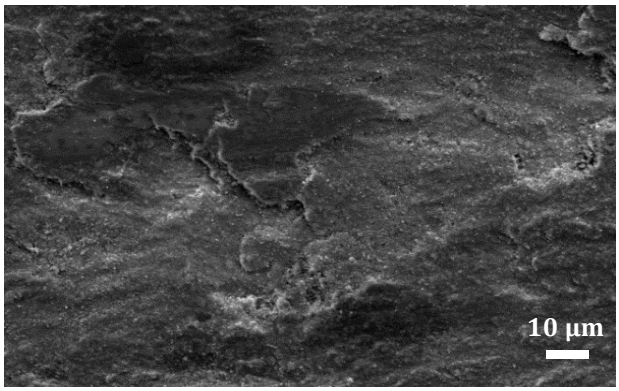

e)

Fig. 6. SEM micrographs showing wear tracks of composite under 5 N applied load (a) SAF 2205 (b) SAF 2205 + 2TiN (c) SAF 2205 + 4TiN (d) SAF 2205 + 6TiN (e) SAF 2205 + 8TiN.

To further elucidate the wear mechanism of the TiN nanoparticle reinforced SAF 2205 composites, SEM-EDX analysis was carried out on the generated wear debris. Figure 7a, b and c revealed the morphologies of the wear debris of duplex and TiN nanoparticles reinforced duplex stainless steel (6 & 8 wt% TiN) respectively collected at the end of the sliding wear tests. During wear test at 1 N applied load, there exist negligible volume of wear debris generated and hence the wear debris were collected at 5 N of applied load to gain insight into the wear mechanisms. The extent of wear in terms of volume of wear debris generated decreased with increase in TiN nanoparticle reinforcement up to 6 wt%. The volume percentage of wear debris also increased due to higher applied loads.

The wear debris morphology generated by duplex stainless steel (Fig. 7a) is in the form of small flakes due to ductile nature. Whereas the steel composite reinforced with 6 wt% TiN nanoparticles composed of agglomerated and fine particles. Debris for the 8 %wt TiN (Fig. 7c) are very fine (instead of flakes) and are generated by work hardened mode rather than ploughing mode due to higher hardness and brittleness of the stainless steel. However, the addition of TiN nanoparticles up to 8 wt% to the matrix alloy results in extremely hard material causing it to be brittle and susceptible to breakage even at low loads [36]. The high TiN content causes the steel material to have high pore volume creating unstable tribolayer, leading to an increase in wear rate. This results in greater penetration of the ball on the composite surface, causing severe plastic deformation and generation of a substantial amount of debris [37]. This degrades the wear resistance as previously discussed and that may be weak interface bonding existing in the duplex matrix and nanoceramic particles. Al Mangour et al. [38] in their work reported that the tribolayer may be damaged by not paying attention to the particle's metallurgy, grain nucleation, and growth.

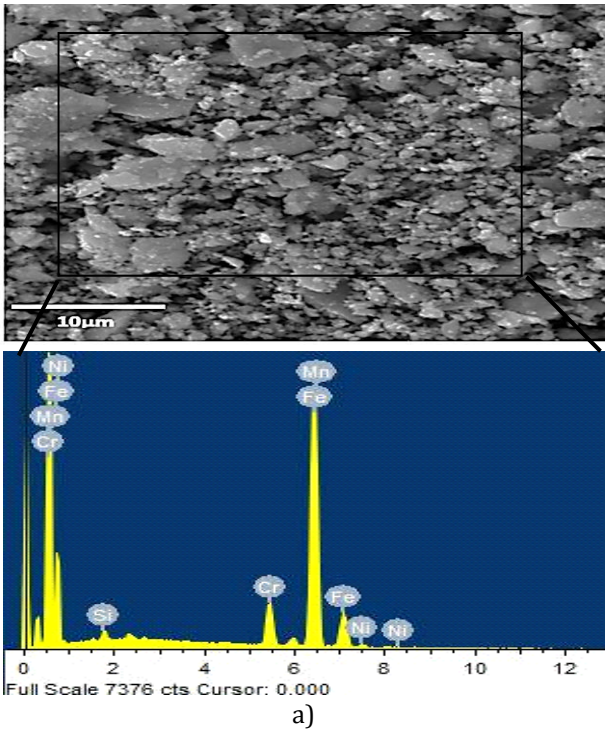

a)

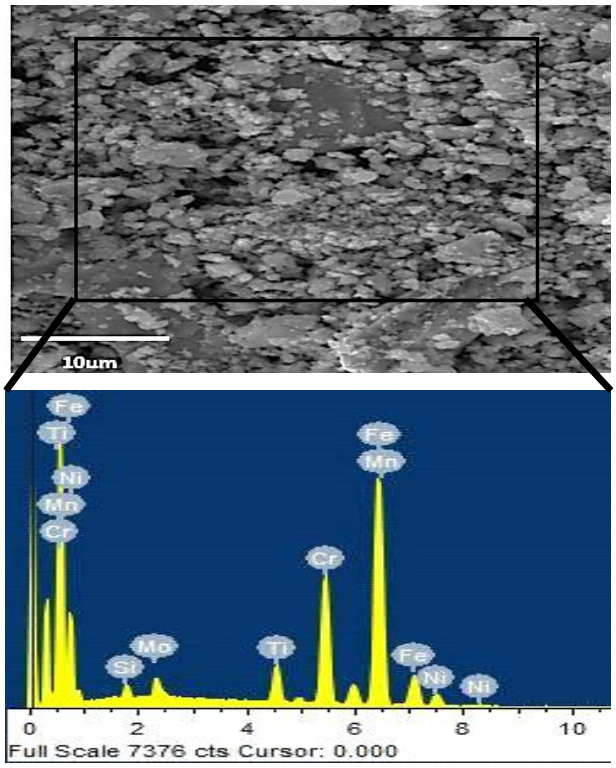

b)

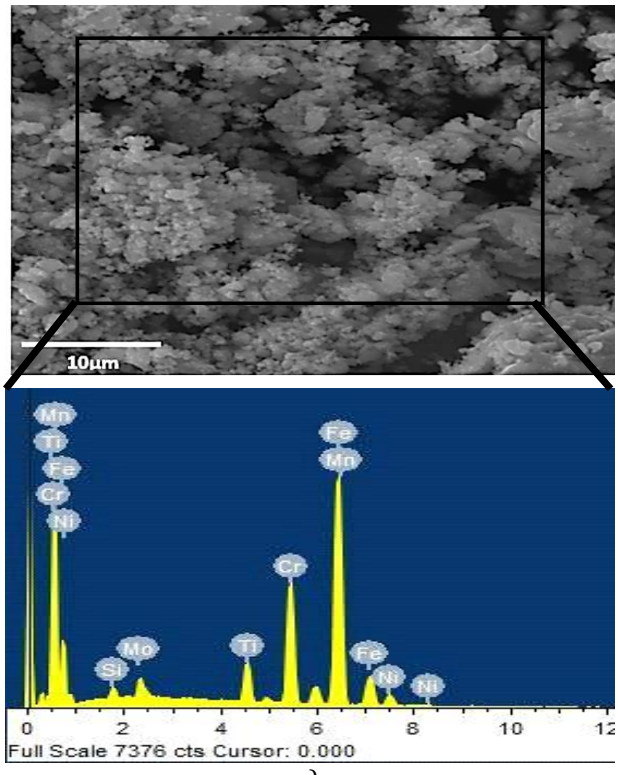

c)

Fig. 7. Wear debris of (a) SAF 2205, (b) SAF 2205 + 6TiN and (c) SAF 2205 + 8TiN generated from sliding wear test under a load of 5N and corresponding EDS.

It is confirmed from the morphologies that both duplex and TiN nanoparticles reinforced stainless steel up to 6 wt% undergoes abrasive wear mechanisms with ploughing and plastic deformation modes respectively while above 6 wt% reinforcement, its adhesive wear mechanisms. The elemental analyses (EDS) of the debris suggest that the steel consisted mainly of Fe, Cr, Ni (Fig. 7a) and Ti due to the TiN nanoparticle addition (Figs. 7b and 7c).

4. DISCUSSION

The results of this study show that an increase in COF occurs with an increase in nanoceramic reinforcement and a decrease in COF with an increase in applied load. In general, friction in metallic contact involves energy dissipation into the system in many forms and one way is in heat generation which resulted in material softening. Afterward, generation of debris is initiated and the stainless steel matrix material is removed from the surface, therefore revealing the reinforcing hard TiN nanoparticles. Consequently, the TiN nanoparticles are pulled out as the bonding between the stainless steel and reinforcement is weakened as the counterface repeatedly slide across the protruding TiN nanoparticles. As the TiN reinforcement increases, there exists a large volume of TiN sliding against the counterface. At this point, virtually all the contacts are provided between the reinforcing TiN nanoparticles and the counter face. This causes the loosened hard TiN particles to act as a third abrasion body which results in a high degree of surface roughness between contacting surfaces and COF increases. Similarly, observation of a rapid increase in COF with an increase in reinforcement content has been reported [39]. It was stated that high porosity levels and agglomerations of reinforcing particle led to the deterioration of wear surface and consequently results in an increase in the COF. The COF of the reinforced samples were higher than that of the unreinforced samples irrespective of the applied load. This indicates that the quality of matrix-reinforcement bonding decreases at higher volumes of reinforcement, resulting in an increase in COF. On the other hand, high applied load induces greater contacts of the components with higher stresses causing flattening of the asperities resulting in less resistance against motion, hence the low COF.

Although COF was high with an increase in reinforcement, increase in wt% of nano TiN resulted in a reduction in the wear volume which

agrees to the statement by Archard and Hirst [40] that wear cannot be directly related to friction. This anti-wear behaviour can be credited to the advantageous restrained grain growth during sintering due to the grain refinement capabilities of TiN. Keeping this in view, it can be suggested that the refined grains of the composite microstructure resulted in a high hardness according to the classical Hall - Petch relationship which states that material hardness is relatively proportional to the grain size. TiN is also characterized by counter material transfer abilities [10] which boosts the nanocomposites anti-wear performance. The role of TiN in grain refinement of SAF 2205 and resistance to plastic deformation parameter H^3/E^2 have been reported in our previous study [41]. Again, the presence of nanoparticles TiN could shield the SAF 2205 matrix from direct contact with the applied load from the counterface. Furthermore, since the nanoparticles are on the composite surface, it causes part of the shear strains built up in the subsurface to get relieved [39]. The anti-wear behaviour was only achieved up to 6 wt% TiN reinforcement, a further increase in nanoparticle led to a decrease in wear resistance. This could be attributed to the deterioration of interfacial bonding between the matrix and reinforcement.

The worn contours revealed that at lower TiN volume fraction, wear was dominated by abrasive wear mechanism which only formed small cuts and ploughing on the composites. This is due to the strengthening effect of TiN nanoparticles on the composites and could be accounted for the reduction in wear. However, at a higher volume fraction of TiN, despite the high hardness conferred by the TiN nanoparticles, high wear volume was found to be surprisingly high. This is likely to be due to the presence of a discontinuity between reinforcement and matrix promoted crack nucleation and propagation due to large volume fractions of TiN promoting delamination process [42]. The delaminated materials are transferred and due to thermal softening of the composites samples, the materials adhered to other sites of the samples during sliding leading to severe cases of wear.

A highlighting point from the above discussion is that consideration of nanograined cermets in the right amount is essential for controlling the behaviour of the nanocomposites. Future research will focus on the effect of sliding speed, sliding distance and higher loads on the composites used in the present study remain objectives to address.

5. CONCLUSION

The effect of nanograined titanium nitride addition on the tribological behaviour of spark plasma sintered SAF 2205 was investigated. The main conclusions were summarized as follows:

1. Unreinforced duplex stainless steel (DSS) has a lower coefficient of friction compared to nanocomposites. Increasing applied load decreased the coefficient of friction.
2. Increasing applied load increased wear volume loss and increase in wt% of nano TiN leads to decrease in the wear volume. An improvement in wear resistance was noted to increase in TiN nanoparticle reinforcements up to 6 wt%.
3. For each of the applied loads, the wear track widths were observed to widen with an increase in TiN nanoparticle reinforcements.
4. Microstructural assessment of the samples revealed a mixed mode of adhesive–abrasive wear mechanisms at lower volume fractions of TiN nanoparticle reinforcement. However, for higher volume fraction of TiN, there is a transition from adhesive–abrasive to adhesive wear mechanism.
5. Fabricated SAF 2205 nanocomposites displayed exceptional wear resistance compared with the pure duplex stainless steel.
6. The morphology of the wear debris suggests that unreinforced DSS and DSS containing 8 wt% of TiN undergoes severe wear. DSS–6 wt% TiN composite is the recommended sample with better wear resistance.

Acknowledgment

This work was supported by the National Research Foundation (NRF), South Africa [grant number 100837].

REFERENCES

[1] I. Zucato, M.C. Moreira, I.F. Machado, S.M.G Lebrao, *Microstructural characterisation and the*

effect of phase transformations on toughness of the UNS S31803 duplex stainless steel aged treated at 850 °C. Materials Research, vol. 5, no. 3, pp. 385-389, 2002, doi: 10.1590/S1516-14392002000300026

[2] S.R. Oke, O.O. Ige, O.E. Falodun, B.A. Obadele, M.R. Mphahlele, P.A. Olubambi, *Dependence of wear and corrosion properties on holding time of spark plasma sintered SAF 2205 reinforced with TiN nanoparticles*, In 2018 IEEE 9th International Conference on Mechanical and Intelligent Manufacturing Technologies (ICMIMT), pp. 80-84, 2018, doi: 10.1109/ICMIMT.2018.8340425

[3] K. Davidson, S. Singamneni, *Selective laser melting of duplex stainless steel powders: An investigation*, Materials & Manufacturing Process, vol. 31, no. 12, pp. 1543-55, 2016, doi: 10.1080/10426914.2015.1090605

[4] S.R. Oke, O.O. Ige, O.E. Falodun, B.A. Obadele, M.R. Mphalele, P.A. Olubambi, *Influence of Sintering Temperature on Hardness and Wear Properties of TiN Nano Reinforced SAF 2205*, In IOP Conference Series: Materials Science and Engineering, vol. 272, no. 1, p. 012030, 2017, doi: 10.1088/1757-899X/272/1/01

[5] C.X. Jin, C.C. Onuoha, Z.N. Farhat, G.J. Kipouros, K.P. Plucknett. *Reciprocating wear behaviour of TiC-stainless steel cermets*, Tribology International, vol. 105, 250-253, 2016, doi: 10.1016/j.triboint.2016.10.012

[6] S.C. Tjong, K.C. Lau, *Sliding wear of stainless steel matrix composite reinforced with TiB_2 particles*, Material Letters, vol. 41, no. 4, pp. 153-158, 1999, doi: 10.1016/S0167-577X(99)00123-8

[7] S.R. Oke, O.O. Ige, O.E. Falodun, M.R. Mphahlele, P.A. Olubambi, *Densification behavior of spark plasma sintered duplex stainless steel reinforced with TiN nanoparticles*, In: IOP Conference Series: Materials Science and Engineering, vol. 430, 012034, 2018, doi: 10.1088/1757-899X/430/1/012034

[8] A. Rokanopoulou, P. Skarvelis, G.D. Papadimitriou, *Microstructure and wear properties of the surface of 2205 duplex stainless steel reinforced with Al2O3 particles by the plasma transferred arc technique*, Surface & Coating Technology, vol. 254, pp. 9376-9381, 2014, doi: 10.1016/j.surfcoat.2014.06.047

[9] H. Engqvist, N. Axén, *Abrasion of cemented carbides by small grits*, Tribology International, vol. 32, no. 9, pp. 527-34, 1999, doi: 10.1016/S0301-679X(99)00084-5

[10] I. Sulima, I. Jawoeska, P. Figiel, *Influence of processing parameters and different content of TiB2 ceramics on properties of composites sintered by high temperature-high pressure (HT-HP) method*, Archives of Metallurgy and Materials, vol. 59, pp. 205-9, 2014, doi: 10.2478/amm-2014-0033

[11] O.E. Falodun, B.A. Obadele, S.R. Oke, O.O. Ige, P.A. Olubambi, M.L. Lethabane, S.W. Bhero, Influence of spark plasma sintering on microstructure and wear behaviour of Ti-6Al-4V reinforced with nanosized TiN. Transactions of Nonferrous Metals Society of China, vol. 28, iss. 1, pp. 47-54, 2018, doi: 10.1016/S1003-6326(18)64637-0

[12] S.R. Oke, O.O. Ige, O.E. Falodun, M.B. Shongwe, P.A. Olubambi, *Optimization of process parameters for spark plasma sintering of nano structured SAF 2205 composite*, J of Mater Res & Tech, vol. 7, no. 2, pp. 126-134, 2018, doi: 10.1016/j.jmrt.2017.03.004

[13] B.L. Bramfit, *The effect of carbide and nitride additions on the heterogeneous nucleation behaviour of liquid iron ion*, Metal Trans, vol. 1, no. 7, pp. 1987-1995, 1970, doi: 10.1007/BF02642799

[14] P.F. Wang, Z. Han, *Friction and wear behaviors of a gradient nano-grained AISI 36L stainless steel under dry and oil-lubricated conditions*, Journal of Material Science & Technology, vol. 34, no. 10, pp. 1835-1842, 2018, doi: 10.1016/j.jmst.2018.01.013

[15] S.R. Oke, O.O. Ige, O.E. Falodun, M.R. Mphahlele, P.A. Olubambi, *Influence of sintering process parameters on corrosion and wear behaviour of SAF 2205 reinforced with nano-sized TiN*, Materials Chemistry & Physics, vol. 206, pp. 166-173, 2018, doi: 10.1016/j.matchemphys.2017.12.018

[16] ASTM G99-05. *Standard test method for wear testing with a pin-on-disk apparatus*, ASTM International, West Conshohocken, PA, 2016, www.astm.org.

[17] M. Buciumeanu, I. Grudu, L. Palaghian, A.S. Miranda, F.S. Silva, *Influence of an additional elastic stress on dry wear behaviour in reciprocating tests*, Tribology International, vol. 42, no. 4, pp. 1101-1107, 2009, doi: 10.1016/j.triboint.2009.03.014

[18] G. Straffelini, A. Molinari, D. Trabucco, *Sliding wear of austenitic and austenitic-ferritic stainless steels*, Metallurgical & Materials Transactions A, vol. 33, no. 3, pp. 613-624, 2002, doi: 10.1007/s11661-002-0123-4

[19] J.K. Lancaster, *The influence of substrate hardness on the formation and endurance of molybdenum disulphide films*, Wear, vol. 10, pp. 103-117, 1967, doi: 10.1016/0043-1648(67)90082-8

[20] C.C. Onuoha, C.X. Jin, Z.N. Farhat, K.P. Plucknett, *The effects TiC grain size and steel binder content on the reciprocating wear behaviour of TiC-316L stainless steel cermets*, Wear, vol. 350-351, pp. 116-129, 2016, doi: 10.1016/j.wear.2016.01.008

[21] Z. Zhang, Y. Chen, L. Zuo, Y. Zhang, Y. Qi, K. Gao, *The effect of volume fraction of WC particles on wear behaviour of in-situ WC/Fe composites by spark plasma sintering,* International Journal of Refractory Metals & Hard Materials, vol. 69, pp. 196-208, 2017, doi: 10.1016/j.ijrmhm.2017.08.009

[22] C.X. Jin, K.P. Plucknett, *Microstructure instability in TiC-316L stainless steel cermets,* International Journal of Refractory Metals & Hard Materials, vol. 58, pp. 74-83, 2016, doi: 10.1016/j.ijrmhm.2016.03.012

[23] Y. Cao, Y.B. Wang, X.H. An, X.Z. Liao, M. Kawasaki, S.P. Ringer, T.G. Langdon, Y.T. Zhu, *Concurrent microstructural evolution of ferrite and austenite in a duplex stainless steel processed by high-pressure torsion*, Acta Materialia, vol. 63, no. 15, pp. 16-29, 2014, doi: 10.1016/j.actamat.2013.09.030

[24] N. Natarajan, S. Vijayarangan, I. Rajendran, *Wear behaviour of A356/25SiCp aluminium matrix composites sliding against automobile friction materials*, Wear, vol. 261, no. 7-8, pp. 812-22, 2006, doi: 10.1016/j.wear.2006.01.011

[25] R.N. Rao, S. Das, D.P. Mondal, G. Dixit, *Dry sliding wear behaviour of cast high strength aluminium alloy (Al-Zn-Mg) and hard particle composites*, Wear, vol. 267, pp. 688-695, 2001, doi: 10.1016/j.wear.2009.06.034

[26] S.M.R Mousavi, S. Abarghouie, S.M. Reihani, Investigation of friction and wear behaviors of *2024 Al/ SiCp composite at elevated temperatures,* J. of Alloys and Compounds, vol. 501, pp. 326-32, 2010, doi: 10.1016/j.jallcom.2010.04.097

[27] H. Wu, J. Zhao, X. Cheng, W. Xia, A. He, J.H. Yun, S. Huang, L. Wang, H. Huang, S. Jiao, Z. Jiang, *Friction and wear characteristics of TiO2 nano-additive water-based lubricant on ferritic stainless steel*, Tribology International, vol. 117, pp. 24-38, 2018, doi: 10.1016/j.triboint.2017.08.011

[28] Z.F. Ni, Y.S. Sun, F. Xue, J. Bai, Y.J. Lu, *Microstructure and properties of austenitic stainless steel reinforced with in situ TiC particulate*, Materials & Design, vol. 32, pp. 1462-1467, 2011, doi: 10.1016/j.matdes.2010.08.047

[29] H.M. Mallikarjuna, C.S. Ramesh, P.G. Kopad, R. Keshavamurthy, D. Sethuram, *Nanoindentation and wear behaviour of copper based hybrid composites reinforced with SiC and MWCNTs synthesized by spark plasma sintering,* Vacuum, vol. 145, pp. 320-333, 2017, doi: 10.1016/j.vacuum.2017.09.016

[30] S.R. Oke, O.O. Ige, O.E. Falodun, A.M. Okoro, M.R. Mphahlele, P.A. Olubambi, *Powder metallurgy of stainless steels and composites: a review of mechanical alloying and spark plasma sintering*, The International Journal of Advanced Manufacturing Technology, pp. 1-20, 2019, doi: 10.1007/s00170-019-03400-2

[31] J. Silvestre, N. Silvestre, J. De Brito, *An overview on the improvement of mechanical properties of ceramics nanocomposites*, Journal of Nanomaterials, p. 3, 2015, doi: 10.1155/2015/106494

[32] B. Niu, X.G. Wang, Z.M. Fan, *Tribology characteristics of ex-situ and in-situ tungsten carbide particles reinforced iron matrix composites produced by spark plasma sintering*, Technol Mater Sci, vol. 28, pp. 449-454, 2013, doi: 10.1016/j.jallcom.2017.02.003

[33] M.A. Chowdhury, M.K. Khalil, D.M. Nuruzzaman, M.L. Rahaman, *The effect of sliding speed and normal load on friction and wear property of aluminium*, Int. J. Mech. Mechatron. Eng, vol. 11, iss. 1, pp. 53-57, 2011, doi: 10.1.1.369.1903

[34] Z. Iqbal, N. Merah, S. Nouari, A.R. Shuaib, N. Al-Aqeeli, *Investigation of wear characteristics of spark plasma sintered W-35 wt%Re alloy and W-25wt%Re-3.2wt%HfC composite*, Tribology International, vol. 116, pp. 129-37, 2017, doi: 10.1016/j.triboint.2017.06.042

[35] O.O. Ajayi, K.C. Ludema, *The effect of microstructure on wear modes of ceramic materials*, Wear, vol. 154, pp. 371-85, 1992, doi: 10.1016/0043-1648(92)90166-6

[36] M.R. Akbarpour, S. Alipour, *Microstructure and tribological properties of nanostructured aluminium reinforced with SiC nanoparticles fabricated by powder metallurgy route*, Transactions of the Indian Institute of Metals, vol. 71, no. 3, pp. 745-52, 2018, doi: 10.1007/s12666-017-1207-6

[37] J. Jiang, F.H. Stott, M.M. Stack, *The role of tribo particulates in dry sliding wear*, Tribology International, vol. 31, no. 5, pp. 245-56, 1998, doi: 10.1016/S0301-679X(98)00027-9

[38] B. AlMangour, D. Grzesiak, J.M. Yang, *In-situ formation of novel TiC particle-reinforced 316L stainless steel bulk-form composites by selective laser melting*, Journal Alloys and Compounds, vol. 706, pp. 409-418, 2017, doi: 10.1016/j.jallcom.2017.01.149

[39] M. Karbalaei Akbari, S. Rajabi, K. Shirvanimoghaddam, H.R. Baharvandi, *Wear and friction behavior of nanosized TiB 2 and TiO 2 particle-reinforced casting A356 aluminum nanocomposites: A comparative study focusing on*

particle capture in matrix, Journal of Composite Materials, vol. 49, iss. 29, pp. 3665-3681, 2015, doi: 10.1177/0021998314568327

[40] J.F. Archard, W. Hirst, *An examination of a mild wear process,* Proceedings of the Royal Society of London, vol. 238, no. 1215, pp. 515-528, 1957, doi: 10.1098/rspa.1957.0015

[41] S.R. Oke, O.O Ige, O.E. Falodun, P.A. Olubambi, J. Westraadt. *Densification and grain boundary nitrides in spark plasma sintered SAF 2205-TiN composite*. International Journal of Refractory Metals and Hard Materials, vol. 81, pp. 78-84 2019, doi: 10.1016/j.ijrmhm.2019.02.021

[42] C.Y.H. Lim, D.K. Leo, J.J.S. Ang, M. Gupta, *Wear of magnesium composites reinforced with nano-sized alumina particles*, Wear, vol. 259, pp. 620-625, 2005, doi: 10.1016/j.wear.2005.02.006